This is an author produced version of a paper published in
Journal of Colloid and Interface Science.
This paper has been peer-reviewed but may not include the final publisher
proof-corrections or pagination.

Access to the published version may require journal subscription.
Published with permission from: Elsevier.

Epsilon Open Archive http://epsilon.slu.se

Phosphate effects on cadmium(II) sorption to ferrihydrite

Charlotta Tiberg[a], Jon Petter Gustafsson,[a,b]*

[a]Department of Soil and Environment, Swedish University of Agricultural Sciences (SLU), Box 7014, SE-750 07 Uppsala, Sweden. C. Tiberg: charlotta.tiberg@slu.se, Tel: +46-18-67 12 24, J.P. Gustafsson: jon-petter.gustafsson@slu.se, Tel: +46-18-67 12 84

[b]Division of Land and Water Resources Engineering, KTH Royal Institute of Technology, SE-100 44 Stockholm, Sweden.

*corresponding author

Highlights

- Phosphate enhances the sorption of cadmium(II) to ferrihydrite.

- Without phosphate present, cadmium(II) predominantly forms inner-sphere bidentate complexes with the ferrihydrite surface.

- The enhanced sorption in systems with phosphate can to a significant extent be explained by the formation of a ternary surface complex.

Abstract

Hypothesis

Phosphate influences the sorption of metals to iron (hydr)oxides. An enhanced formation of inner-sphere complexes on the (hydr)oxide surface can be attributed to electrostatic interactions and/or to changes in metal coordination on the iron (hydr)oxide surface. Phosphate was expected to enhance cadmium(II) sorption on ferrihydrite. It should be possible to identify changes in cadmium(II) coordination upon phosphate addition by Extended X-ray absorption fine structure (EXAFS) spectroscopy and implement the identified complexes in a surface complexation model.

Experiments

The effect of phosphate addition on cadmium(II) sorption to ferrihydrite was studied by a series of batch experiments covering the pH range from 4 to 8. EXAFS spectroscopy was performed on ferrihydrite from the batch experiments at the cadmium(II) K edge. The identified surface complexes were incorporated in the Charge distribution multisite complexation (CD-MUSIC) model, and new surface complexation constants were optimized.

Findings

Without phosphate addition cadmium(II) formed inner-sphere bidentate complexes on the ferrihydrite surface. With phosphate there was an increased cadmium(II) sorption that could not be explained by electrostatic interactions alone. The enhancement was best explained by the formation of a ternary complex including cadmium(II), phosphate and ferrihydrite surface groups.

1.   Introduction

Cadmium is a toxic element. Cadmium has chemical properties similar to zinc, an essential nutrient, and a reason for its toxicity is probably the displacement of essential zinc in proteins [1]. Anthropogenic emissions during the 20th century has caused elevated cadmium concentrations in, for example, the humus layer of Swedish forest soils [2] and sites contaminated by historical industrial activities such as production of nickel-cadmium-batteries. The use of cadmium-containing phosphate fertilizers has led to increased cadmium levels in agricultural soils and crops. The average cadmium concentration in the Earth's crust is 0.15 mg kg^{-1} [3] and the concentration in unpolluted natural water is usually <0.1 µg L^{-1} [4]. The World Health Organization drinking water guideline for cadmium is 3 µg L^{-1} [5].

To predict transport, bioavailability and toxicity of metals in soil it is crucial to understand their distribution between different soil compartments, especially as the total concentration of a metal in soil is usually not directly related to its mobility or uptake in organisms. Rather, mobility, bioavailability and toxicity are controlled by the speciation of the metal. Despite many studies on cadmium binding to soil and soil constituents [6] there are still important knowledge gaps regarding cadmium speciation in soil. The interactions between cadmium(II) and phosphorus in soils is one example. Several studies show a decreased cadmium mobility in soils after the addition of different forms of phosphate [7]. On the other hand an increase of cadmium mobility was the result of bone-meal addition to a contaminated soil [8]. At high concentrations of cadmium and phosphate the immobilization of cadmium is primarily due to the precipitation of cadmium phosphates [9]. At lower concentrations the major immobilization mechanism is probably increased sorption to soil constituents induced by the increase in negative surface charge caused by adsorbed phosphate, and possibly also the formation of surface complexes including both cadmium and phosphate [7]. In the case of the

increased cadmium mobility after bone-meal addition, the results could be explained by the high pH in the treated soil, which prevented the dissolution of apatite, and by cadmium(II) complexation with organic acids released due to the bone meal treatment [8].

It is well known that cadmium(II) forms strong complexes with both organic matter and metal (hydr)oxides [10-12]. Complexation to organic matter and soil (hydr)oxides is strongly pH-dependent and increases with increasing pH. Cadmium(II) forms inner-sphere complexes on iron (hydr)oxides. EXAFS (Extended X-ray absorption spectroscopy) investigations indicate the formation of bidentate edge-sharing complexes with Cd⋯Fe distance ~3.3 Å and bidentate corner-sharing complexes with Cd⋯Fe distance 3.5 Å or 3.7 Å [11, 13]. Parkman et al. [14] interpreted the presence of a 3.7 Å Cd⋯Fe distance as evidence for a monodentate complex. Both bidentate and monodentate complexes have been used in surface complexation models (SCM) to describe cadmium(II) sorption to ferrihydrite and goethite [15-17].

The sorption of metals to iron (hydr)oxides often increases in the presence of phosphate [18, 19]. This is also true for sorption of cadmium(II) ions on iron (hydr)oxides [17, 20], but there is no consistency as to the causes of the enhancement. Venema et al. [17] attributed the enhanced cadmium(II) sorption to goethite to electrostatic effects and to the increasing importance of a monodentate complex after phosphate addition. Elzinga and Kretzschmar [21] identified ternary cadmium(II)-phosphate-hematite surface complexes by ATR-FTIR (Attenuated total reflectance Fourier transform infrared spectroscopy), but Collins et al. [22] excluded the formation of ternary cadmium(II)-phosphate-goethite complexes as they were not able to identify any Cd⋯P distances in their EXAFS analysis.

In this work we studied the interactions between cadmium(II) and an iron (hydr)oxide (ferrihydrite) in the absence and presence of phosphate. The aims were to study how phosphate affects the sorption of cadmium(II) to ferrihydrite, to identify the cadmium(II) complexes formed

and to derive surface complexation constants. The cadmium(II) concentrations reflect slightly/moderately contaminated soils based on the Swedish classification of contaminated soils [23], and the results are important to understand how cadmium(II) interacts with iron (hydr)oxide surfaces in, for example, iron-rich cadmium(II)-contaminated soils.

2.   Materials and methods

2.1   Ferrihydrite preparation

2-line ferrihydrite was prepared using the method of Schwertmann and Cornell [24]. A solution containing 36 mmol L^{-1} $Fe(NO_3)_3$ and 12 mmol L^{-1} $NaNO_3$ was brought to pH 8.0 through drop-wise addition of 4 mol L^{-1} NaOH (prepared immediately before use). The resulting suspension was aged for about 16 h at $20^{o}C$. Ferrihydrite particles from such a suspension have earlier been examined by Fe K-edge EXAFS spectroscopy [25] and found to consist of 2-line ferrihydrite. After synthesis, the ferrihydrite suspension was back-titrated with 0.1 mol L^{-1} HNO_3 to pH 4.6. The suspension was then stirred for about 30 min before starting the batch experiments, to avoid the presence of excessive CO_2 in the suspensions.

2.2   Batch experiments

Series of 30 mL batches were prepared in 40 mL polypropylene centrifuge tubes. There were three series with cadmium(II) and ferrihydrite containing 3 mmol L^{-1} ferrihydrite and 0.3, 3 or 30 μmol L^{-1} cadmium(II), and one series with 0.3 mmol L^{-1} ferrihydrite and 30 μmol L^{-1} cadmium(II). The ionic strength and pH of the ferrihydrite suspensions were adjusted by adding appropriate amounts of $NaNO_3$, HNO_3 and/or NaOH (prepared the same day) to cover a pH range of about 4 to 8 and to give a final NO_3^- concentration of 0.01 mol L^{-1}. Additional series were prepared with addition of phosphate; 600 μmol L^{-1} to the systems with 3 mmol L^{-1}

ferrihydrite, and 60 µmol L^{-1} to the systems with 0.3 mmol L^{-1} ferrihydrite. Phosphate was

added as NaH_2PO_4, directly followed by the addition of $Cd(NO_3)_2$ from an 1.5 mM stock

solution. The samples were equilibrated on an end-over-end shaker, and shaken gently for 24 h at

room temperature (21°C). They were then centrifuged for 20 min at about 3000g. The pH was

measured on the unfiltered supernatant using a Radiometer combination electrode. The rest of

the suspension was filtered using 0.2-µm single-use filters (Acrodisc PF, Pall Corporation, Ann

Arbor, MI). Part of the filtered suspension was acidified (1% HNO_3) and analyzed for Cd with

inductively coupled plasma mass spectroscopy (ICP-MS) using a Perkin-Elmer ELAN 6100

instrument (Perkin-Elmer Inc., Waltham, MA, USA). Dissolved phosphate concentrations were

analyzed on filtered samples with the acid molybdate method using flow injection analysis

(Aquatec-Tecator Autoanalyzer, Foss Analytical, Copenhagen).

Two additional series of batches were prepared and analyzed in the same way except that

the phosphate was replaced by arsenate. The purpose was to verify that arsenate and phosphate

affect the cadmium(II) sorption in the same way. If so, arsenate could be used as an analogue for

phosphate in some EXAFS measurements to facilitate the interpretation of the results (see

Methods section about EXAFS). Arsenate was added as Na_2HAsO_4, and analysis of As in the

supernatant was made in the same way as for cadmium.

The adsorption of cadmium(II) to filters and container walls was investigated by

equilibrating 3 µmol L^{-1} cadmium(II) solutions without ferrihydrite on an end-over-end shaker

for 24 h. Results showed between 7.7 and 9.5% cadmium(II) adsorption in the pH range of 5.9 to

6.5. Batch results were not corrected for this effect. Concerning the possible effect of $CO_2(g)$ on

the results, Tiberg et al. [19] determined dissolved inorganic carbon (DIC) in batch experiments

with 3 mmol L^{-1} ferrihydrite and with no metals added in the pH range of 4 to 10. The results

were used to evaluate DIC effects on cadmium(II) sorption (see section 2.5 on geochemical modeling).

2.3   EXAFS measurements

Ferrihydrite from batch experiments with the two highest Cd/Fe ratios were analyzed with EXAFS spectroscopy. The samples were centrifuged once more after removal of the supernatant to increase the cadmium(II) concentration. An EXAFS spectrum of a solution standard, 15 mmol L^{-1} Cd(NO$_3$)$_2$, was also collected.

One difficulty when studying interactions with phosphorus by EXAFS spectroscopy is that phosphorus is a light element and therefore contributes little to the EXAFS signal from higher shells. Arsenate has sorption properties similar to phosphate. However, arsenic is heavier than phosphorus and therefore easier to identify by EXAFS. It is also possible to do complementary EXAFS measurements on the arsenic K edge, whereas EXAFS measurements on phosphorus K edge are very difficult. A few ferrihydrite samples in which phosphate had been substituted for arsenate were therefore prepared to study the coordination of cadmium(II).

EXAFS measurements at the Cd K edge were performed at beamline B18, Diamond Light Source, UK. Measurements on the cadmium(II) solution standard were made at beamline X-11A at the National Synchrotron Lightsource (NSLS), Brookhaven laboratory, US. Arsenic K edge EXAFS spectra were collected at beamline 4-1 at the Stanford Synchrotron Radiation Lightsource (SSRL), US. Measurements were performed in fluorescence mode and internal energy calibration was made with a foil of metallic cadmium assigned to 26,711 eV or with a metallic arsenic foil assigned to 11,867 eV [26]. The monochromator was detuned about 50% to reduce higher order harmonics and about 10 scans were collected per sample. Beamline B18 at the Diamond Light Source operated at 3.0 GeV and with a ring current of 300 mA (top-up

mode). The station was equipped with a Si[311] double crystal monochromator and a 9-element Ge fluorescence detector. Palladium filters and Soller slits were placed between the sample and the detector to reduce iron fluorescence and scattering contributions. Beamline X-11A at NSLS operated at 2.5 GeV with a ring current of 200 mA and electrons injected every 12 hours. The station was equipped with a Si[311] double crystal monochromator and a PIPS detector. A Palladium filter was used. Beamline 4-1 at SSRL operated at 3.0 GeV and with a ring current of 197-200 mA (top-up mode). The station was equipped with a Si[220] double crystal monochromator and a 13 element Ge fluorescence detector. A germanium filter and an aluminum foil were placed between the sample and the detector to reduce contributions from Fe fluorescence.

2.4   EXAFS data treatment

All EXAFS spectra were treated in the Athena software (version 0.8.061) [27]. Energy calibration, averaging and background removal were performed according to the procedures described by Kelly et al. [28]. The background was removed using the AUTOBAK algorithm incorporated in Athena with a *k*-weight of two or three for the background function and Rbkg = 1 for cadmium and Rbkg = 0.85 for arsenic.

Wavelet transform (WT) analysis of the EXAFS spectra was performed [29] to differentiate between light (e.g. O) and heavy (e.g. Fe) back-scatterers in higher shells. This qualitative analysis of back-scattering contributions from higher-shell atoms was performed on k^3-weighted EXAFS spectra with the Morlet WT incorporated in the Igor Pro script [30] with the parameter combination $\kappa = 7$ and $\sigma = 1$ and a range of $R + \Delta R$ from 2 to 4 Å (corresponding to interatomic distances of about 2.5 to 4.5 Å). The *k*-ranges were the same as in the EXAFS fitting procedure.

The Artemis program (version 0.0.012) [27] was used for final data treatment of the EXAFS spectra. Theoretical scattering paths were calculated with FEFF6 [31]. The amplitude reduction factor (S_0^2) was set based on fitting of the first coordination shell. Several combinations of scattering paths were tested in the fitting procedure before deciding what paths to use. These included contributions from Cd–O, Cd···Fe, Cd···P and Cd···As distances as well as multiple scattering paths.

Values of CN were chosen to give reasonable values of σ^2. The Cd···Fe paths used in the final fits were based on the mineral structure of keyite [32] with partial Cu for Fe and Zn for Cd substitution and monteponite [33] with partial Fe-for-Cd substitution. The Cd···P path was based on NaCdPO$_4$ [34], the Cd···As path on NaCdAsO$_4$ [35] and the As···Fe path on scorodite [36]. Fitting was performed on the Fourier transform real part between 1 and 4 Å using a Hanning window (dk value = 1) and optimizing over k-weights of 1, 2 and 3. Refined models were evaluated by means of goodness-of-fit of the Fourier Transform (as evidenced by the R factor in Artemis) and qualitative comparison of WT plots of the model spectra with WT plots of the EXAFS spectra. WT of the model spectra were made with the same WT-parameters and k-ranges as for measured spectra.

2.5 *Geochemical modeling*

Cadmium(II) surface complexation to ferrihydrite was simulated with the CD-MUSIC (Charge distribution multisite complexation) model [37] in the Visual MINTEQ 3.1 software [38] with the surface charging parameters of Tiberg et al. (2013). The surface complex-forming ions (Cd^{2+}, PO_4^{3-}, AsO_4^{3-}) were assumed to react exclusively with the ≡FeOH groups, as these are generally considered to be the most reactive ones (Hiemstra et al., 2009). All surface complexation reactions considered are listed in Table 1. Model simulations with DIC concentrations measured

by Tiberg et al., [19] showed a very small effect of DIC on cadmium(II) sorption (the cadmium(II) sorption increased <0.6%). DIC was therefore not considered in the modeling.

For phosphate and arsenate adsorption, the model description assumes bidentate complexes to predominate. A doubly protonated monodentate species was also included but was only found to be of some importance at low pH [39, 40]. Phosphate surface complexation constants were optimized by Tiberg et al. [19], and arsenate surface complexation constants by Gustafsson (unpublished), based on the arsenate binding data sets treated by Gustafsson and Bhattacharya [39].

The surface complexation reactions for cadmium(II) were constrained from the spectroscopic evidence of this study (c.f. Results). The SCM of the series with only cadmium and ferrihydrite was improved by the introduction of surface site heterogeneity. The sorption sites were divided into two groups with different affinities for cadmium(II) ion adsorption, so that 1% of the total number of sites was assigned a higher adsorption affinity than the remaining 99%.

For ternary systems, i.e. for ferrihydrite suspensions that contained both cadmium(II) and phosphate or arsenate, initial model predictions were made assuming that any ternary interactions could be explained with electrostatic interactions only. A second modeling attempt included a ternary complex based on interpretation of EXAFS measurements (c.f. Results section). Consideration of site heterogeneity for the ternary complexes did not improve the model fits. Therefore, site heterogeneity was only used for Cd-ferrihydrite complexes in the final model.

In the model optimization process, surface complexation constants for a given reaction were optimized with PEST [41], which is integrated with Visual MINTEQ. PEST uses a Gauss-Marquardt-Levenberg algorithm for parameter estimation and minimizes the weighted sum of

squared differences between model-generated observation values and the measured values. The CD values were optimized by trying different (reasonable) combinations of values for the o-plane and b-plane and comparing the correlation coefficient R, which is the goodness-of-fit value reported by PEST. Generally R should be >0.9 for an acceptable fit. The 95% confidence intervals of the surface complexation constants were calculated by PEST.

Table 1. Surface complexation reactions and constants used in the CD-MUSIC model for ferrihydrite-cadmium(II).

Reaction	$(\Delta z_0, \Delta z_1, \Delta z_2)^a$	$\log K^b$	Data source(s)
$FeOH^{\frac{1}{2}-} + H^+ \leftrightarrow FeOH_2^{\frac{1}{2}+}$	(1,0,0)	8.1	[c]
$Fe_3O^{\frac{1}{2}-} + H^+ \leftrightarrow Fe_3OH^{\frac{1}{2}+}$	(1,0,0)	8.1	Assumed the same as above
$FeOH^{\frac{1}{2}-} + Na^+ \leftrightarrow FeOHNa^{\frac{1}{2}+}$	(0,1,0)	-0.6	Hiemstra & van Riemsdijk (2006)
$Fe_3O^{\frac{1}{2}-} + Na^+ \leftrightarrow Fe_3ONa^{\frac{1}{2}+}$	(0,1,0)	-0.6	”
$FeOH^{\frac{1}{2}-} + H^+ + NO_3^- \leftrightarrow FeOH_2NO_3^{\frac{1}{2}-}$	(1,-1,0)	7.42	”
$Fe_3O^{\frac{1}{2}-} + H^+ + NO_3^- \leftrightarrow Fe_3OHNO_3^{\frac{1}{2}-}$	(1,-1,0)	7.42	”
$2FeOH^{\frac{1}{2}-} + 2H^+ + PO_4^{3-} \leftrightarrow Fe_2O_2PO_2^{2-} + 2H_2O$	(0.46,-1.46,0)	27.59	Tiberg et al (2013)
$2FeOH^{\frac{1}{2}-} + 3H^+ + PO_4^{3-} \leftrightarrow Fe_2O_2POOH^- + 2H_2O$	(0.63,-0.63,0)	32.89	”
$FeOH^{\frac{1}{2}-} + 3H^+ + PO_4^{3-} \leftrightarrow FeOPO_3H_2^{\frac{1}{2}-} + H_2O$	(0.5,-0.5,0)	30.22	”
$2FeOH^{\frac{1}{2}-} + 2H^+ + AsO_4^{3-} \leftrightarrow Fe_2O_2AsO_2^{2-} + 2H_2O$	(0.47,-1.47,0)	27.36	Gustafsson (unpubl)
$2FeOH^{\frac{1}{2}-} + 3H^+ + AsO_4^{3-} \leftrightarrow Fe_2O_2AsOOH^- + 2H_2O$	(0.58,-0.58,0)	32.42	”
$FeOH^{\frac{1}{2}-} + 3H^+ + AsO_4^{3-} \leftrightarrow FeOAsO_3H_2^{\frac{1}{2}-} + H_2O$	(0.5,-0.5,0)	29.5	”
$2FeOH^{\frac{1}{2}-} + Cd^{2+} + H_2O \leftrightarrow (FeOH)_2CdOH + H^+$	(0.5,0.5,0)	-1.42 (99%)^d	This study
	(0.5,0.5,0)	1.31 (1%)^d	”
$2FeOH^{\frac{1}{2}-} + 2H^+ + Cd^{2+} + PO_4^{3-} \leftrightarrow (FeO)_2HCdPO_3H^0 + H_2O$	(0.7,0.3,0)	30.50^d	”
$2FeOH^{\frac{1}{2}-} + 2H^+ + Cd^{2+} + AsO_4^{3-} \leftrightarrow (FeO)_2HCdAsO_3H^0 + H_2O$	(0.7,0.3,0)	30.01^d	”

[a] The change of charge in the o-, b- and d-planes respectively.
[b] Two numbers indicate binding to sites with different affinity, the percentages of which are within brackets (c.f. text).
[c] The log K values of the singly- and triply-coordinated surface groups were set equal in line with Hiemstra and van Riemsdijk [37] and the values correspond to the point-of zero charge of ferrihydrite [42].
[d] 95% confidence intervals calculated by PEST; -1.42 +/- 0.15, 1.31 +/- 0.2, 30.50 +/- 0.06, 30.01 +/- 0.06.

3.   Results and discussion

3.1   *Effect of phosphate and arsenate on cadmium(II) adsorption to ferrihydrite*

The cadmium(II) sorption increased with increasing pH from about 0% at low pH to 100% at high pH (Fig 1). At low surface coverage (Cd/Fe ratio about 0.0001-0.001) the amount of cadmium(II) sorbed was close to the results from earlier studies of cadmium(II) sorption to ferrihydrite [15, 43], although the sorption edges reported in this study are somewhat steeper. However, at higher surface coverage (Cd-Fe ratio about 0.001-0.01), the sorption was stronger in this study than in the earlier studies. The differences may be due to differences in the synthesized ferrihydrite.

The sorption edge was displaced to higher pH with increasing Cd/Fe-ratio in systems with only cadmium(II) and ferrihydrite (Fig 1a). This indicates that cadmium(II) sorption, as in earlier work [15, 43], depends on the surface loading and suggests the presence of sites with different affinities for cadmium(II) sorption. With phosphate added the sorption was independent of the surface loading except at the highest Cd/Fe ratio (0.1) where the surface approaches saturation (Fig 1b). The sorption edge was then displaced to higher pH due to competition for sorption sites. The sorption of phosphate and arsenate decreased with increasing pH (Fig 2).

12
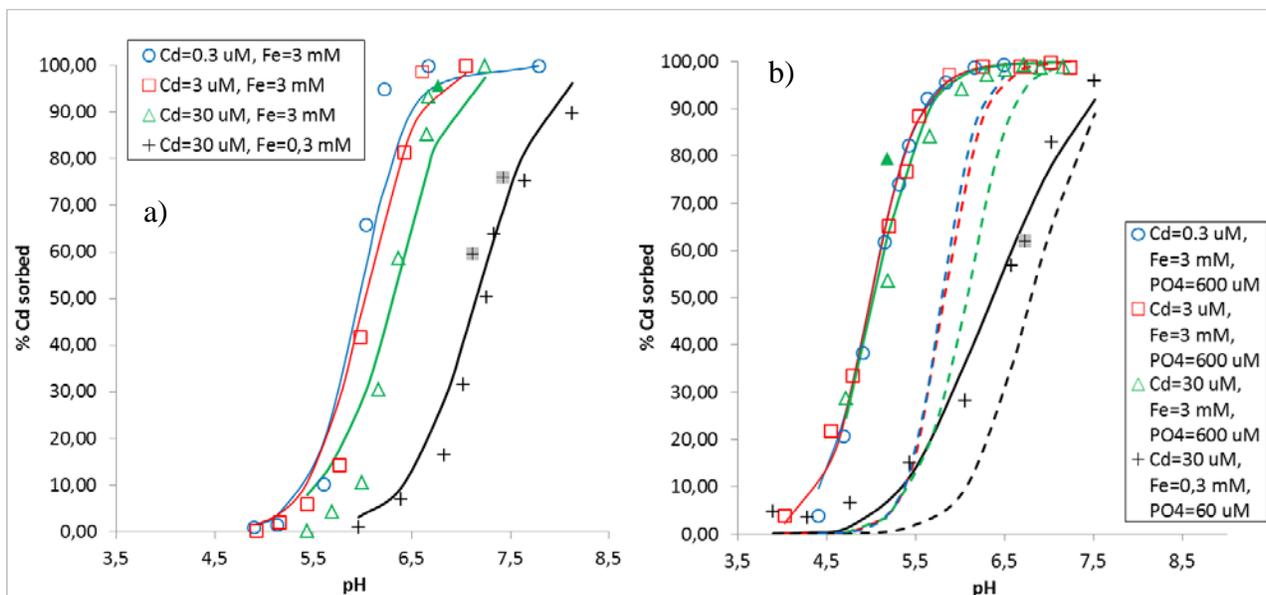
Fig 1. Cadmium(II) sorption to ferrihydrite at Cd/Fe ratios 0.0001, 0.001, 0.01 and 0.1. Results from batch experiments (symbols) and SCM (lines) with the optimized parameters from Table 1. Filled symbols are samples for EXAFS measurements. a) Only cadmium(II) and ferrihydrite. b) With phosphate added; model without ternary surface complex (dashed lines) and with ternary complex (solid lines).
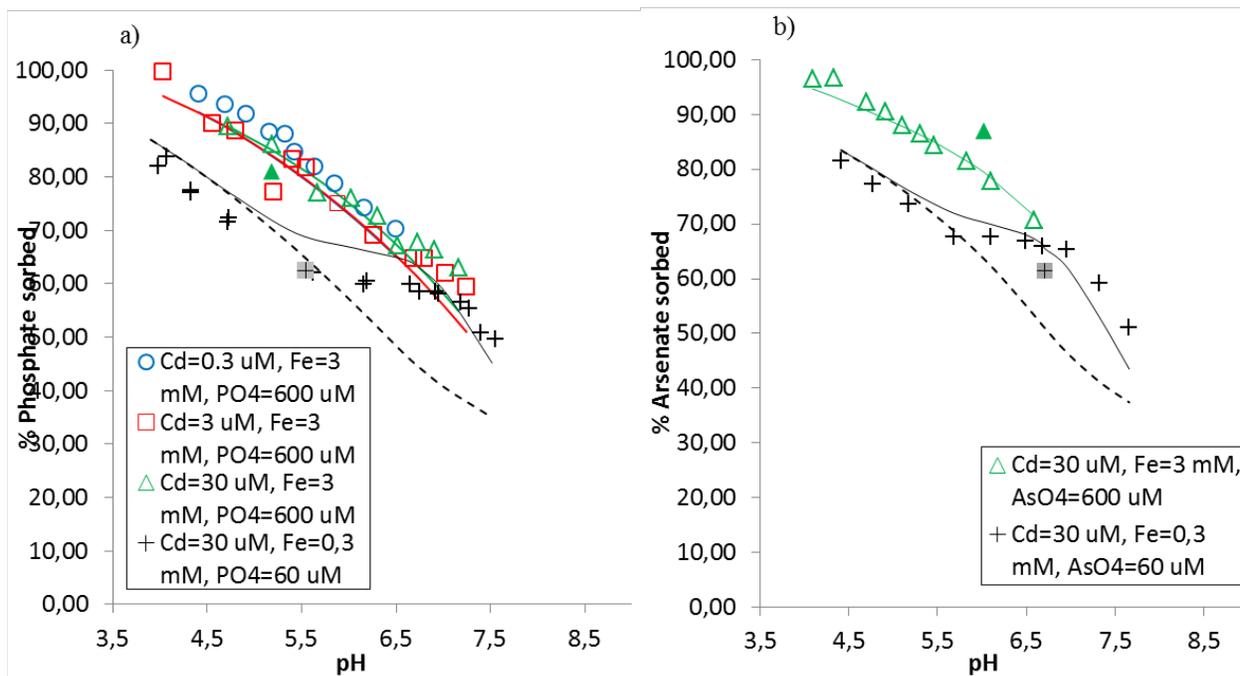
Fig 2.Sorption of phosphate and arsenate to ferrihydrite (symbols). Lines are results from SCM with the optimized parameters of Table 1. Solid lines are simulations with a ternary complex and dashed lines are series with 30 μM Cd, 0.3 mM Fe and 60 μM PO_4/AsO_4 without a ternary complex. Filled symbols are samples for EXAFS measurements a) Phosphate, b) Arsenate.

13

Phosphate increased cadmium(II) sorption at all Cd/Fe ratios, i.e. more cadmium(II) was adsorbed at a certain pH in batches with phosphate added (Fig 3). The addition of arsenate produced results very similar to those with phosphate (Fig 3).

Significant formation of cadmium(II) precipitates was excluded, as all suspensions were undersaturated with respect to $Cd(OH)_2(s)$, $Cd_3(PO_4)_2(s)$ and $Cd_3(AsO_4)_2(s)$ according to calculations in Visual Minteq.
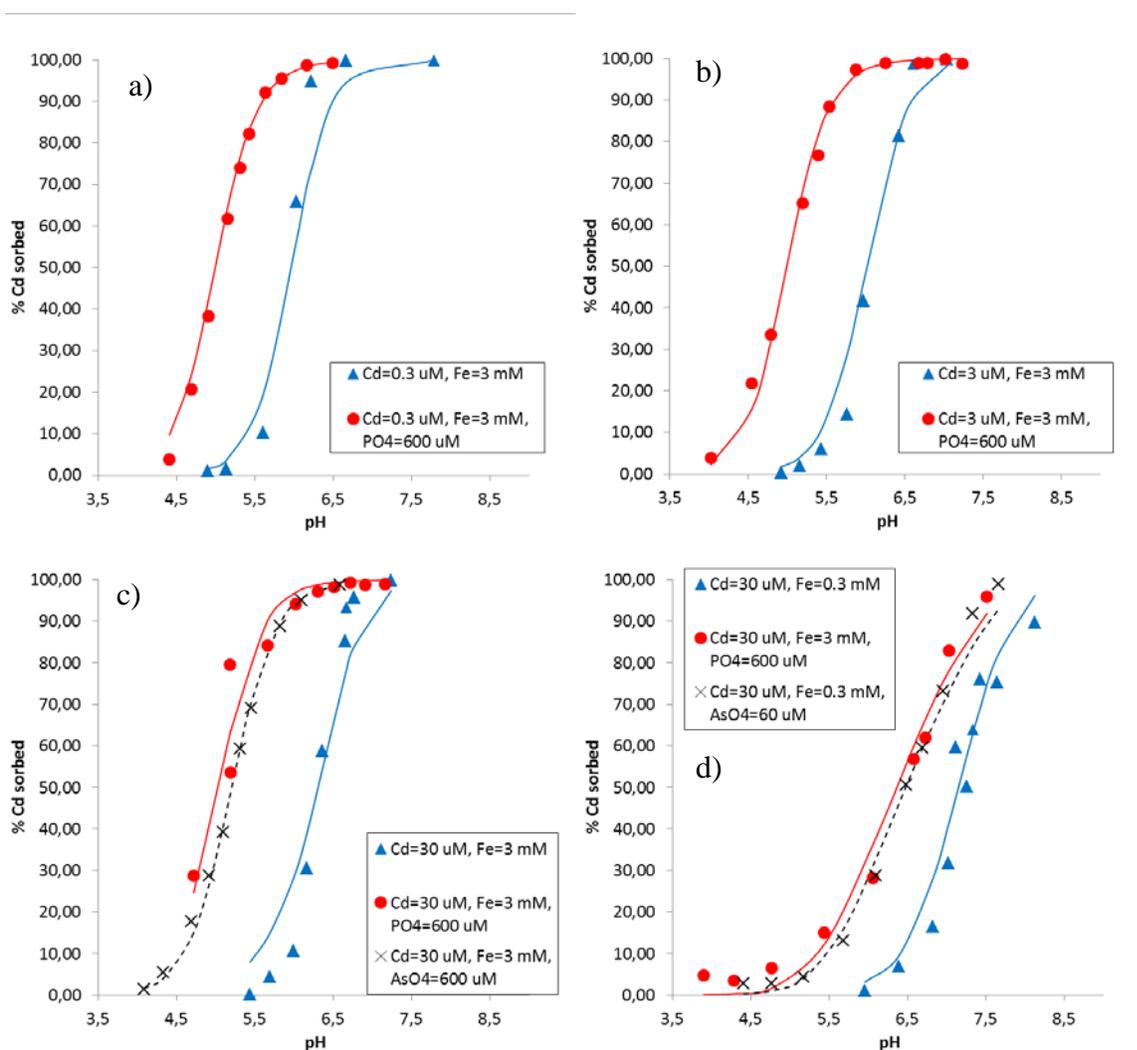
Fig 3. Sorption of cadmium(II) to ferrihydrite (blue symbols), with phosphate added (red symbols) and with arsenate added (black symbols). Lines are SCM results with the optimized parameters from Table 1. a) Cd/Fe ratio 0.0001, b) Cd/Fe ratio 0.001, c) Cd/Fe ratio 0.01 and d) Cd/Fe ratio 0.1.

3.2   Structure of cadmium surface complexes on ferrihydrite

To elucidate the structure of the cadmium(II) surface complexes formed, nine ferrihydrite samples were analyzed with EXAFS spectroscopy (Table 2). A spectrum of dissolved $Cd(NO_3)_2$ (Fig 4) was also collected. A visual comparison of these spectra revealed that the cadmium(II) coordination changed when phosphate or arsenate was added. The spectra with only ferrihydrite and cadmium(II) were more asymmetric than the spectrum for the $Cd(NO_3)_2$ solution standard (i. e. the marked area in Fig 4), while the spectra from samples with phosphate or arsenate were more similar in shape to the $Cd(NO_3)_2$ spectrum.

A detailed picture of the complexes formed was obtained from models of the EXAFS spectra (Table 2). In all samples cadmium(II) was coordinated to six oxygens at a distance of 2.26-2.27 Å in the first shell. Possible contributions from higher shells were identified in the WT analysis. There were distinct differences between samples with and without phosphate/arsenate. With only cadmium(II) and ferrihydrite present, the high intensity of the WT modulus indicated back-scatterers heavier than oxygen at $k \approx 7$ and $R = 2.7$ to 3.5 Å (not phase-shifted, Fig S1, Supplementary material). This signal was reduced in samples with phosphate or arsenate added (Fig S2 and S3, Supplementary material). EXAFS spectra from samples without added anions were best fit with two different Cd···Fe distances (Table 2). Both distances can be interpreted as evidence for the formation of bidentate complexes where the 3.3 Å distance is an edge-sharing and 3.7 Å a corner-sharing complex (Fig. 5A, 5B) [11, 22]. A 3.7 Å Cd···Fe distance has also been interpreted as a bent monodentate complex [14]. Higher-shell contributions in phosphate-containing samples were best fit with a Cd···Fe distance at about 3.8 Å and a Cd···P distance at about 3.4 Å. Similarly, samples with arsenate were best fit with a Cd···Fe distance at 3.8 Å and with a Cd···As distance at about 3.5 Å. The low intensity of the WT modulus in the WT plots of

these samples is explained by interferences between the Cd···Fe and the Cd···P or Cd···As

distances.

Table 2. Summary of cadmium and arsenic K-edge EXAFS shell fit results[a]. Parameters in italics were constrained during fitting. Error bars of fitted parameters within brackets.

Sample	Path	CN	R (Å)	σ^2 (Å^2)	ΔE (eV)	S_0^2	R-factor (%)
Cd(aq)	Cd–O	*6*	2.27 (0.01)	0.008 (0.000)	0.70 (0.62)	*1*	0.7
Cd(NO$_3$)$_2$(aq)	Cd-O-O[c]	*18*	4.43 (0.03)	*0.017*			
15 mM	Cd-O···O[d]	*24*	3.72 (0.10)	*0.025*	k-range 3.0-10.0		
H 2 pH=6.67	Cd–O	*6*	2.26 (0.01)	0.009 (0.001)	-0.64 (0.59)	*0.75*	0.6
30 µM Cd,	Cd···Fe1	*0.5*	3.24 (0.04)	0.007 (0.006)			
3 mM Fe	Cd···Fe2	*1*	3.78 (0.03)	0.007 (0.005)			
	Cd-O-O[b]	*18*	4.55 (0.05)	*0.019*	k-range 2.6-9.5		
H 6 pH=7.12	Cd–O	*6*	2.27 (0.01)	0.010 (0.001)	-0.40 (0.61)	*0.75*	0.6
30 µM Cd,	Cd···Fe1	*0.5*	3.26 (0.06)	0.008 (0.008)			
0.3 mM Fe	Cd···Fe2	*1*	3.76 (0.04)	0.007 (0.005)			
	Cd-O-O[b]	*18*	4.53 (0.05)	*0.018*	k-range 2.6-9.5		
H 7 pH=7.42	Cd–O	*6*	2.26 (0.01)	0.009 (0.001)	-0.37 (0.61)	*0.75*	0.7
30 µM Cd,	Cd···Fe1	*0.5*	3.26 (0.05)	0.006 (0.006)			
0.3 mM Fe	Cd···Fe2	*1*	3.74 (0.04)	0.006 (0.005)			
	Cd-O-O[b]	*18*	4.55 (0.05)	*0.018*	k-range 2.6-9.5		
H 3 pH=5.18	Cd–O	*6*	2.27 (0.01)	0.010 (0.001)	-0.30 (0.54)	*0.85*	0.4
30 µM Cd,	Cd···P	*1*	3.36 (0.07)	0.017 (0.011)			
3 mM Fe,	Cd···Fe2	*1*	3.81 (0.08)	0.017 (0.012)			
600 µM P	Cd-O-O[b]	*18*	4.50 (0.04)	*0.020*	k-range 2.6-9.5		
H 8 pH=6.73	Cd–O	*6*	2.27 (0.01)	0.010 (0.000)	-0.10 (0.47)	*0.85*	0.4
30 µM Cd,	Cd···P	*1*	3.38 (0.04)	0.012 (0.007)			
0.3 mM Fe,	Cd···Fe2	*1*	3.80 (0.05)	0.013 (0.008)			
60 µM P	Cd-O-O[b]	*18*	4.50 (0.04)	*0.020*	k-range 2.6-9.5		
H 10 pH=6.02	Cd–O	*6*	2.27 (0.01)	0.009 (0.000)	-0.87 (0.45)	*0.85*	0.3
30 µM Cd,	Cd···As	*1*	3.45 (0.08)	0.014 (0.010)			
3 mM Fe,	Cd···Fe2	*1*	3.74 (0.08)	0.013 (0.010)			
600 uM As	Cd-O-O[b]	*18*	4.47 (0.04)	*0.019*	k-range 2.6-9.5		
H 12 pH=6.71	Cd–O	*6*	2.27 (0.01)	0.009 (0.000)	0.09 (0.46)	*0.80*	0.4
30 µM Cd,	Cd···As	*1*	3.51 (0.10)	0.014 (0.014)			
0.3 mM Fe,	Cd···Fe2	*1*	3.77 (0.07)	0.010 (0.010)			
60 µM As	Cd-O-O[b]	*18*	4.48 (0.04)	*0.019*	k-range 2.6-9.5		
H 12b pH=6.72	As–O	*4*	1.69 (0.01)	0.001 (0.000)	1.07 (1.62)	*0.80*	1.6
60 µM As,	As-O···O[b]	*12*	3.07 (0.04)	*0.002*			
0.3 mM Fe,	As···Fe	*1*	3.33 (0.04)	0.010 (0.004)			
30 µM Cd					k-range 3.6-12.5		
I 11 pH=7.05	As–O	*4*	2.27 (0.01)	0.002 (0.000)	-0.76 (1.78)	*0.90*	1.8
60 µM As	As-O···O[b]	*12*	3.06 (0.05)	*0.004*			
0.3 mM Fe,	As···Fe	*1*	3.30 (0.07)	0.009 (0.003)	k-range 3.6-12.5		

[a] CN = Coordination number; R = Atomic distance; σ^2 = Debye-Waller factor; ΔE = Energy shift parameter; S_0^2 = Passive amplitude reduction factor; R-factor = goodness-of-fit parameter of the Fourier Transform; sum of the squares of the differences between the data and the fit at each data point, divided by the sum of the squares of the data at each corresponding point. In general, R-factor values less than 5% are considered to reflect a reasonable fit. The error bars of fitted parameters (within brackets) are given as in Artemis [27].
[b] For each sample the ss(Å^2) of Cd-O-O (multiple scattering path 180°) were defined as 2*ss(Å^2) for the Cd-O paths.
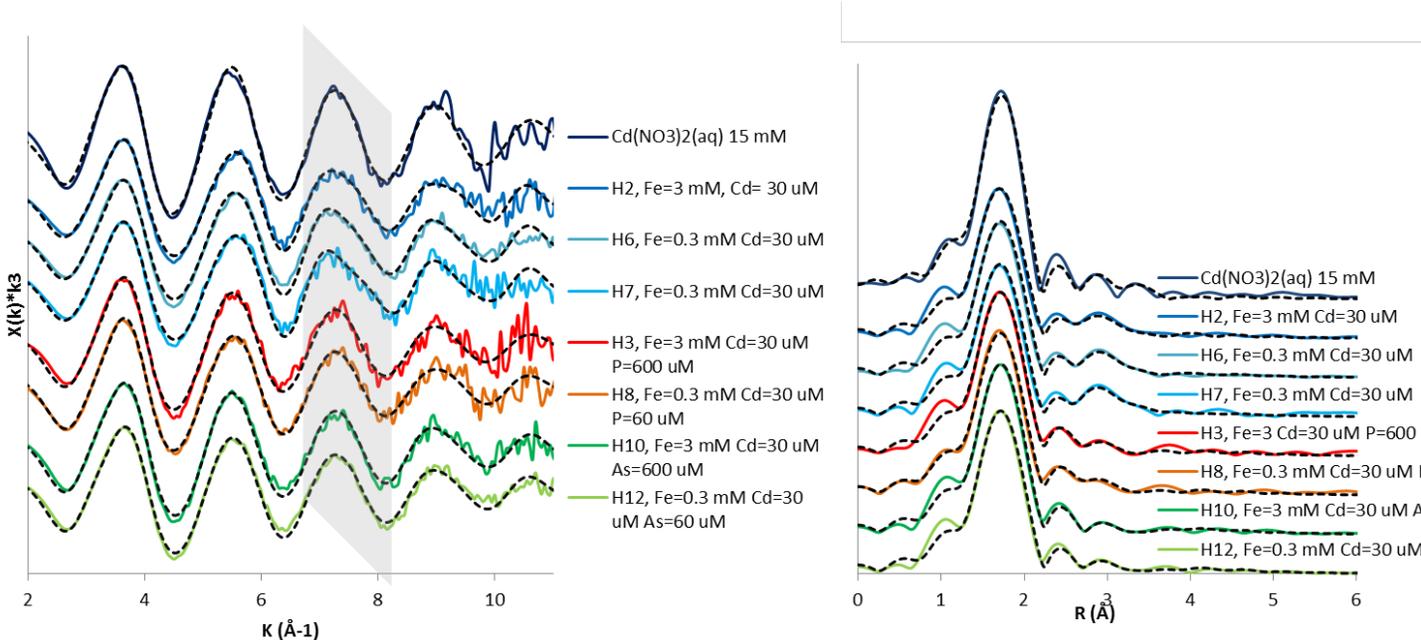
Fig 4. Results from EXAFS measurements of cadmium(II) adsorbed to ferrihydrite and $Cd(NO_3)_2$ solution. a) EXAFS spectra (solid lines) and model fits (dashed lines). b) Fourier transforms of EXAFS spectra (soild lines) and model fits (dashed lines). The shaded area highlights an area where spectra for sample H2, H6 and H7 have a different shape than spectra from H3, H10 and H12.

The distances identified in the samples with phosphate and arsenate are consistent with the formation of a ternary complex including a cadmium(II) ion, a phosphate or arsenate ion, and the ferrihydrite surface. Possible arrangements of such a complex that are consistent with our EXAFS interpretations are depicted in Fig. 5C-D. Cadmium(II) may coordinate to both the ferrihydrite surface and to phosphate or arsenate (Fig 5C or 5D). Cadmium(II) and phosphate have been proposed to form similar complexes on hematite based on ATR-FTIR measurements [21].

A. Edge-sharing
(FeOH)$_2$CdOH

B. Corner-sharing
(FeOH)$_2$CdOH

C. Ternary
(FeOH)2CdPO$_4$H$_2^0$

D. Ternary
(FeO)$_2$HCdPO$_3$H^0
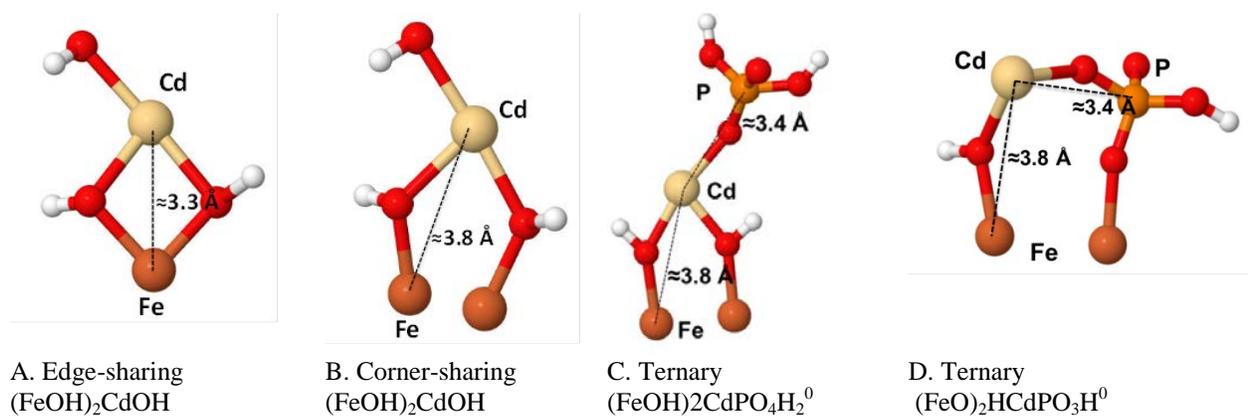
Fig 5. Structures of cadmium(II) surface complexes consistent with both EXAFS interpretations and SCM results. Bright red atoms are oxygen and white atoms are hydrogen. Iron, cadmium(II) and phosphorus atoms are marked. The Cd···Fe and Cd···P distances from the EXAFS analysis are shown. Structures of the ternary cadmium(II)-arsenate complexes are similar except that the Cd···As distance is 3.5 Å.

For the arsenate-containing sample with the highest Cd/As ratio (sample H12), arsenic K-edge EXAFS spectroscopy was performed. A reference spectrum with only arsenate and ferrihydrite was collected for comparison (Table 2, Fig S5, Supplementary material). The arsenic K-edge EXAFS spectra with and without cadmium(II) were very similar and the arsenic was concluded to be present mainly as arsenate ions coordinated to two iron atoms of the ferrihydrite surface (corner-sharing complexes) with As···Fe distance 3.3 Å [44, 45]. The WT plots are presented in Fig S5, Supplementary material. An As···Cd distance could not be identified, probably because the contribution was too weak in comparison to the signal from the 3.3 Å As···Fe distance. This was supported by results from SCM according to which most of the arsenic was coordinated only to iron also in the sample with cadmium.

3.3   SCM for cadmium(II) sorption to ferrihydrite

The cadmium(II) adsorption reaction in the single sorbate system could, based on the EXAFS

analysis, be understood as the formation of bidentate complexes. (The SCM used does not

distinguish between edge- and corner-sharing complexes). The best modeling results were

obtained with a hydrolyzed cadmium(II) complex (Fig 1a) and inclusion of a high-affinity site

constituting 1% of the sorption sites (c.f Methods section). All surface complexation reactions

are listed in Table 1. The fitted CD-MUSIC values were 0.5 for both the *o*- and the *b*-plane,

which means that a fraction (*f*) of 0.25 of the Cd^{2+} charge was attributed to the surface, which is

reasonable.

Cadmium(II) sorption in samples with phosphate added was poorly described by the

model developed for the cadmium(II)-ferrihydrite system (Fig 1b). This model predicted an

increase in cadmium(II) sorption caused by electrostatic effects but could only explain a small

part of the increase in cadmium(II) sorption. The ternary complexes depicted in Fig 5

(complexes C, D) were consistent with EXAFS measurements and could both be described by

the same surface complexation reaction, in which two surface groups on the ferrihydrite react

with one cadmium(II) ion and one phosphate or arsenate ion (Table 1). The addition of

$\equiv(FeO)_2HCdPO_3H^0$ and $\equiv(FeO)_2HCdAsO_3H^0$ complexes to the SCM and subsequent

optimization of the surface complexation constants resulted in much better agreement with

experimental data (Fig 1b). The CD values for the ternary complex were 0.7 for the *o*-plane and

0.3 for the *b*-plane. This resulted in $f = 0.24$, which is very close to the value of the bidentate Cd-

ferrihydrite complex. Other divalent metals have been suggested to form similar complexes

under the same experimental conditions [19]. The model with ternary complexes also simulated

the sorption of phosphate and arsenate better than the model without any ternary complexes (Fig.

2). With a ternary complex the model could simulate the "plateau" in the series with the lowest

19

P/Cd and As/Cd ratio. In the series with higher phosphate addition (600 µM) there was no visible effect of the ternary complexes due to the much higher concentrations of phosphate compared to cadmium(II). Ternary complexes have earlier been used in geochemical models of cadmium(II) sorption to ferrihydrite and goethite in presence of sulphate [15], but this is the first time a SCM has used ternary complexes to describe cadmium(II) sorption to ferrihydrite in the presence of phosphate.

4.   Conclusions

Phosphate greatly enhanced cadmium(II) sorption to ferrihydrite. The increased sorption could not be explained by electrostatic interactions alone. A ternary ferrihydrite-cadmium(II)-phosphate surface complex had to be considered. This study confirmed our hypotheses that phosphate would enhance cadmium(II) sorption to ferrihydrite and that it should be possible to identify the surface complexes formed by EXAFS spectroscopy and implement these complexes in a SCM.

Previous studies have shown increased sorption of cadmium(II) to iron (hydr)oxides in the presence of phosphate, but only to goethite [17, 20]. Our study is also the first to identify ternary iron (hydr)oxide-cadmium(II)-phosphate surface complexes by EXAFS spectroscopy and to successfully implement such complexes in a SCM, the CD-MUSIC model. In contrast to earlier EXAFS measurements of cadmium(II) sorbed to goethite in presence of phosphate [22] we identified a Cd···P distance indicative of a ternary complex at about 3.4 Å by EXAFS. The existence of a ternary complex was supported by an earlier ATR-FTIR analysis of a cadmium(II)-phosphate-hematite system [21].

The results indicate that phosphate increases cadmium(II) sorption to ferrihydrite in soils. This is potentially an important retention mechanism for cadmium(II) in iron-rich soils and could

affect risk assessments of contaminated soils. The results could also be useful in the development of new remediation strategies using phosphate and iron (hydr)oxides for remediation of contaminated soils and groundwater. Future work on cadmium(II) sorption to soils with different levels of phosphorus and iron (hydr)oxides is needed to clarify when phosphorus has an influence on the overall cadmium(II) mobility in soils.

RERERENCES

[1] G.W. Buchko, N.J. Hess, M.A. Kennedy, Cadmium mutagenicity and human nucleotide excision repair protein XPA: CD, EXAFS and (1)H/(15)N-NMR spectroscopic studies on the zinc(II)- and cadmium(II)-associated minimal DNA-binding domain (M98-F219), Carcinogenesis, 21 (2000) 1051-1057.

[2] K. Johansson, B. Bergbäck, G. Tyler, Impact of atmospheric long range transport of lead, mercury and cadmium on the Swedish forest environment, Water Air Soil Pollut. Focus, 1 (2001) 279-297.

[3] M. Winter, Source: WebElements http://www.webelements.com/, http://www.webelements.com/, Accessed 5 Jan 2016.

[4] G.F. Nordberg, B.A. Fowler, M. Nordberg, Handbook on the Toxicology of Metals, Academic Press, 2014.

[5] World_Health_Organization, Guideline for drinking-water quality, fourth edition, 2011.

[6] P. Loganathan, S. Vigneswaran, J. Kandasamy, R. Naidu, Cadmium sorption and desorption in soils: a Review, Crit. Rev. Environ. Sci. Technol., 42 (2012) 489-533.

[7] N.S. Bolan, D.C. Adriano, P. Duraisamy, A. Mani, K. Arulmozhiselvan, Immobilization and phytoavailability of cadmium in variable charge soils. I. Effect of phosphate addition, Plant Soil, 250 (2003) 83-94.

[8] I.R. Sneddon, M. Orueetxebarria, M.E. Hodson, P.F. Schofield, E. Valsami-Jones, Field trial using bone meal amendments to remediate mine waste derived soil contaminated with zinc, lead and cadmium, Appl. Geochem., 23 (2008) 2414-2424.

[9] N. Siebers, J. Kruse, P. Leinweber, Speciation of phosphorus and cadmium in a contaminated soil amended with bone char: sequential fractionations and XANES spectroscopy, Water Air Soil Pollut., 224 (2013) 1564.

[10] T. Karlsson, K. Elgh-Dalgren, E. Bjorn, U. Skyllberg, Complexation of cadmium to sulfur and oxygen functional groups in an organic soil, Geochim. Cosmochim. Acta, 71 (2007) 604-614.

[11] S.R. Randall, D.M. Sherman, K.V. Ragnarsdottir, C.R. Collins, The mechanism of cadmium surface complexation on iron oxyhydroxide minerals, Geochim. Cosmochim. Acta, 63 (1999) 2971-2987.

[12] R.M. Floroiu, A.P. Davis, A. Torrents, Cadmium adsorption on aluminum oxide in the presence of polyacrylic acid, Environ. Sci. Technol., 35 (2001) 348-353.

[13] L. Spadini, A. Manceau, P.W. Schindler, L. Charlet, Structure and stability of Cd^{2+} surface complexes on ferric oxides: 1. Results from EXAFS spectroscopy, J. Colloid Interface Sci., 168 (1994) 73-86.

[14] R.H. Parkman, J.M. Charnock, N.D. Bryan, F.R. Livens, D.J. Vaughan, Reactions of copper and cadmium ions in aqueous solution with goethite, lepidocrocite, mackinawite, and pyrite, Am. Miner., 84 (1999) 407-419.

[15] P.J. Swedlund, J.G. Webster, G.M. Miskelly, The effect of SO_4 on the ferrihydrite adsorption of Co, Pb and Cd: ternary complexes and site heterogeneity, Appl. Geochem., 18 (2003) 1671-1689.

[16] P.J. Swedlund, J.G. Webster, G.M. Miskelly, Goethite adsorption of Cu(II), Pb(II), Cd(II), and Zn(II) in the presence of sulfate: properties of the ternary complex, Geochimica Et Cosmochimica Acta, 73 (2009) 1548-1562.

[17] P. Venema, T. Hiemstra, W.H. van Riemsdijk, Interaction of cadmium with phosphate on goethite, J. Colloid Interface Sci., 192 (1997) 94-103.

[18] T.E. Payne, J.A. Davis, T.D. Waite, Uranium adsorption on ferrihydrite - effects of phosphate and humic acid, Radiochim. Acta, 74 (1996) 239-243.

[19] C. Tiberg, C. Sjöstedt, I. Persson, J.P. Gustafsson, Phosphate effects on copper(II) and lead(II) sorption to ferrihydrite, Geochim. Cosmochim. Acta, 120 (2013) 140-157.

[20] K. Wang, B. Xing, Adsorption and desorption of cadmium by goethite pretreated with phosphate, Chemosphere, 48 (2002) 665-670.

[21] E.J. Elzinga, R. Kretzschmar, In situ ATR-FTIR spectroscopic analysis of the co-adsorption of orthophosphate and Cd(II) onto hematite, Geochim. Cosmochim. Acta, 117 (2013) 53-64.

[22] C.R. Collins, K.V. Ragnarsdottir, D.M. Sherman, Effect of inorganic and organic ligands on the mechanism of cadmium sorption to goethite, Geochim. Cosmochim. Acta, 63 (1999) 2989-3002.

[23] Swedish Environmental Protection Agency, Methods for inventories of contaminated sites, Report 5053, 1st edition, Stockholm, Sweden, 2002.

[24] U. Schwertmann, R.M. Cornell, Iron oxides in the laboratory: preparation and characterization, Weinheim, Wiley, 2000.

[25] J.P. Gustafsson, I. Persson, D.B. Kleja, J.W.J. van Schaik, Binding of iron(III) to organic soils: EXAFS spectroscopy and chemical equilibrium modeling, Environ. Sci. Technol. 41 (2007), 1232-1237.

[26] A. Thompson, D. Attwood, E. Gullikson, M. Howells, K.-J. Kim, J. Kirtz, J. Kortright, I. Lindau, Y. Liu, P. Pianetta, A. Robinson, J. Scofield, J. Underwood, G. Williams, H. Winck, X-ray Data Booklet, Lawrence Berkeley National Laboratory, University of California, Berkeley, California, 2009.

[27] B. Ravel, M. Newville, ATHENA, ARTEMIS, HEPHAESTUS: data analysis for X-ray absorption spectroscopy using IFEFFIT, J. Synchrotron Rad., 12 (2005) 537-541.

[28] S. Kelly, D. Hesterberg, B. Ravel, Analysis of soils and minerals using X-ray absorption spectroscopy, in: A.L. Ulery, R.L. Drees (Eds.) Methods of soil analysis. Part 5. Mineralogical methods, SSSA Book Series, SSSA, Madison, WI, 2008.

[29] H. Funke, A. Scheinost, M. Chukalina, Wavelet analysis of Extended X-ray absorption fine structure data, Phys. Rev. B, 71 (2005) 094110.

[30] M. Chukalina, Wavelet2.ipf, a procedure for calculating the Wavelet transform in IGOR Pro, http://www.esrf.eu/UsersAndScience/Experiments/CRG/BM20/Software/Wavelets/IGOR, 2010.

[31] S.I. Zabinsky, J.J. Rehr, A. Ankudinov, R.C. Albers, M.J. Eller, Multiple-scattering calculations of x-ray-absorption spectra, Phys. Rev. B, 52 (1995) 2995-3009.

[32] M.A. Cooper, F.C. Hawthorne, The crystal structure of keyite, Can. Miner., 34 (1996) 623-630.

[33] J. Zhang, Crystal Structure of monteponite, Phys. Chem. Miner., 26 (1999) 644-648.

[34] Y.A. Ivanov, M.A. Simonov, N.V. Belov, NaCd[PO$_4$], triphylite-analogue, Kristallogr., 19 (1974) 163-164.

[35] M. Weil, Olivine-type NaCd(AsO$_4$), Acta Crystallogr. Sect. E, E69 (2013).

[36] Y. Xu, G.-P. Zhou, X.-F. Zheng, Redetermination of iron(III) arsenate dihydrate, Acta Crystallogr. Sect. E, 63 (2007) i67-i69.

[37] T. Hiemstra, W.H. van Riemsdijk, A surface structural approach to ion adsorption: The charge distribution (CD) model, J. Colloid Interface Sci., 179 (1996) 488-508.

[38] J.P. Gustafsson, Visual MINTEQ 3.1, http://vminteq.lwr.kth.se/, 2013.

[39] J.P. Gustafsson, P. Bhattacharya, Geochemical modelling of arsenic adsorption to oxide surfaces, In: P. Bhattacharya, A.B. Mukherjee, J. Bundschuh, R. Zevenhoven, R.H. Loeppert (Eds.) Trace Metals and other Contaminants in the Environment, Elsevier, 2007, pp. 159-206.

[40] C. Sjöstedt, T. Wällstedt, J.P. Gustafsson, H. Borg, Speciation of aluminium, arsenic and molybdenum in excessively limed lakes, Sci. Total Environ., 407 (2009) 5119-5127.

[41] J. Doherty, PEST. Model-idependent parameter estimation. User manual, 5th edition., Watermark Numerical Computing. , Web: http://www.pesthomepage.org, 2010.

[42] D.A. Dzombak, F.M.M. Morel, Surface complexation modeling - hydrous ferric oxide, John Wiley and Sons, New York, 1990.

[43] M.M. Benjamin, J.O. Leckie, Multiple-site adsorption of Cd, Cu, Zn, and Pb on amorphous iron oxyhydroxide, J. Colloid Interface Sci., 79 (1981) 209-221.

[44] D.M. Sherman, S.R. Randall, Surface complexation of arsenic(V) to iron(III) (hydr)oxides: structural mechanism from ab initio molecular geometries and EXAFS spectroscopy, Geochim. Cosmochim. Acta, 67 (2003) 4223-4230.

[45] A. Manceau, The mechanism of anion adsorption on iron oxides: Evidence for the bonding of arsenate tetrahedra on free $Fe(O, OH)_6$ edges, Geochim. Cosmochim. Acta, 59 (1995) 3647–3653.

Supplementary material

Phosphate effects on cadmium(II) sorption to ferrihydrite

Charlotta Tiberg, Jon Petter Gustafsson

Table of Contents
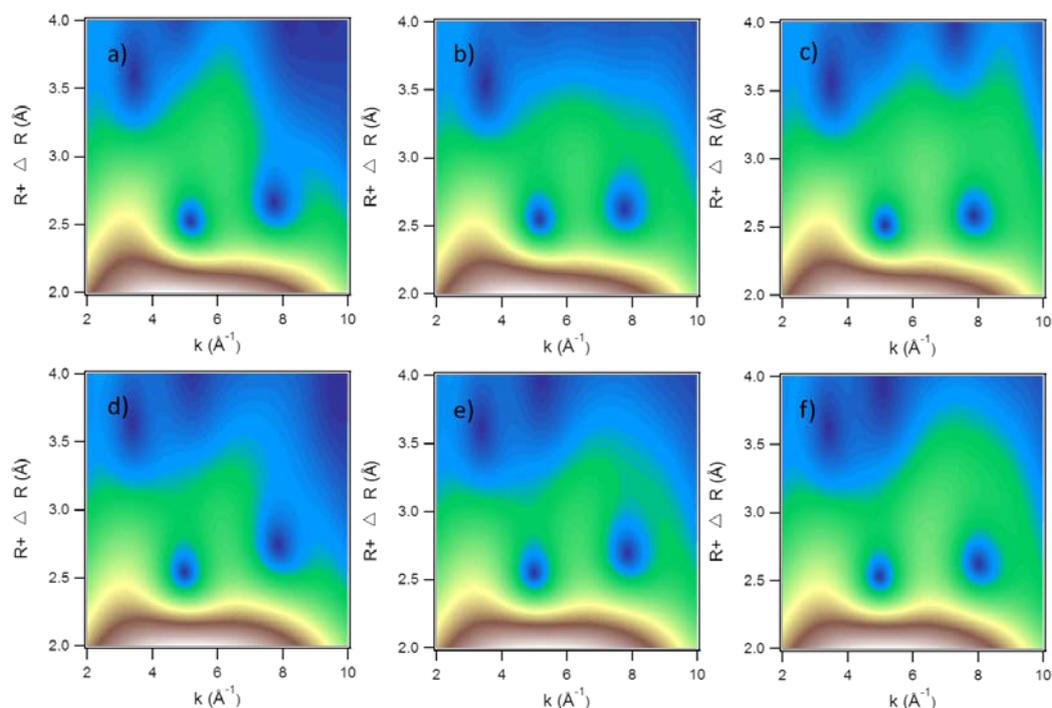
Fig S1. Wavelet transforms of EXAFS spectra and models for cadmium(II) bound to ferrihydrite. The k-range used was 2.6-9.5 Å^{-1}. a) Spectrum H2; 30 µmol L^{-1} Cd, 3 mmol L^{-1} Fe, b) Spectrum H6; 30 µmol L^{-1} Cd, 0.3 mmol L^{-1} Fe, c) Spectrum H7; 30 µmol L^{-1} Cd, 0.3 mmol L^{-1} Fe, d) Model H2, e) Model H6, f) Model H7.
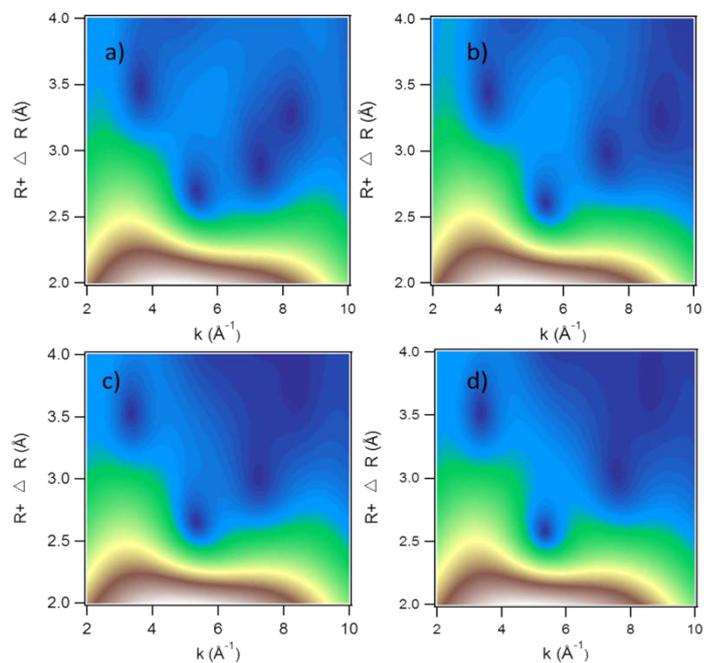
Fig S2. Wavelet transforms of spectra and models Cd(II) bound to ferrihydrite with phosphate added. The *k*-range used was 2.6-9.5 Å^{-1} for all samples. a) Spectrum H3; 30 µmol L^{-1} Cd, 3 mmol L^{-1} Fe, 600 µM P, b) Spectrum H8; 30 µmol L^{-1} Cd, 0.3 mmol L^{-1} Fe, 60 µmol L^{-1} P, c) Model H3, d) Model H8.
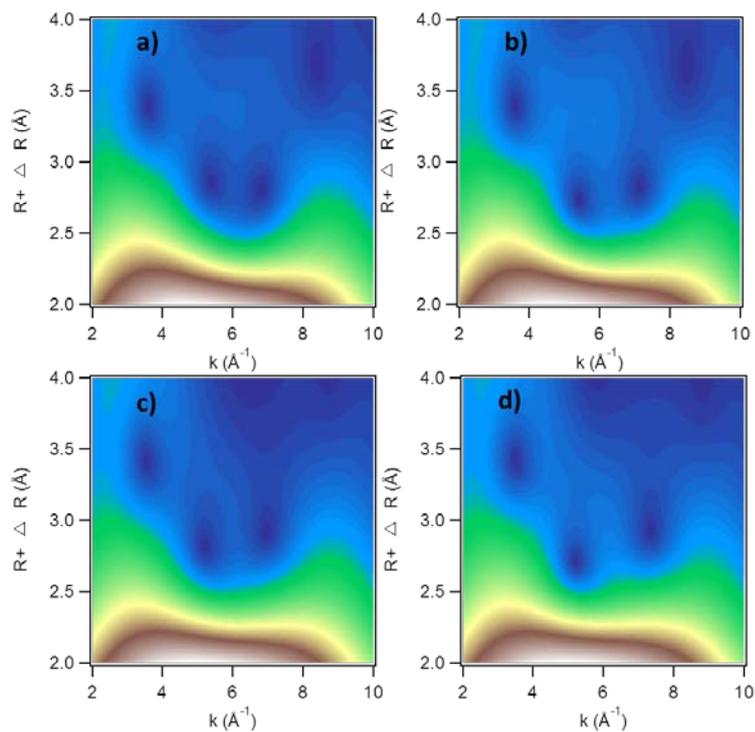
Fig S3. Wavelet transforms of spectra and models Cd(II) bound to ferrihydrite with arsenate added. The *k*-range used was 2.6-9.5 Å^{-1} for all samples. a) Spectrum H10; 30 µmol L^{-1} Cd, 3 mmol L^{-1} Fe, 600 µmol L^{-1} As, b) Spectrum H12; 30 µmol L^{-1} Cd, 0.3 mmol L^{-1} Fe, 60 µmol L^{-1} As, c) Model H10, d) Model H12.
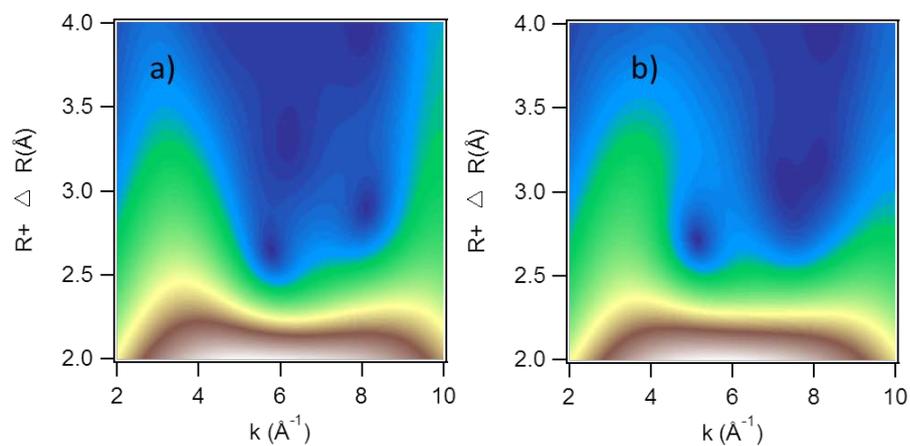
Fig S4. Wavelet transform of EXAFS spectra and model for cadmium(II) solution a) Spectrum 15 mmol L^{-1} Cd(NO3)2(aq), b) Model 15 mmol L^{-1} Cd(NO3)2(aq), The k-range used was 3-10 Å^{-1}.
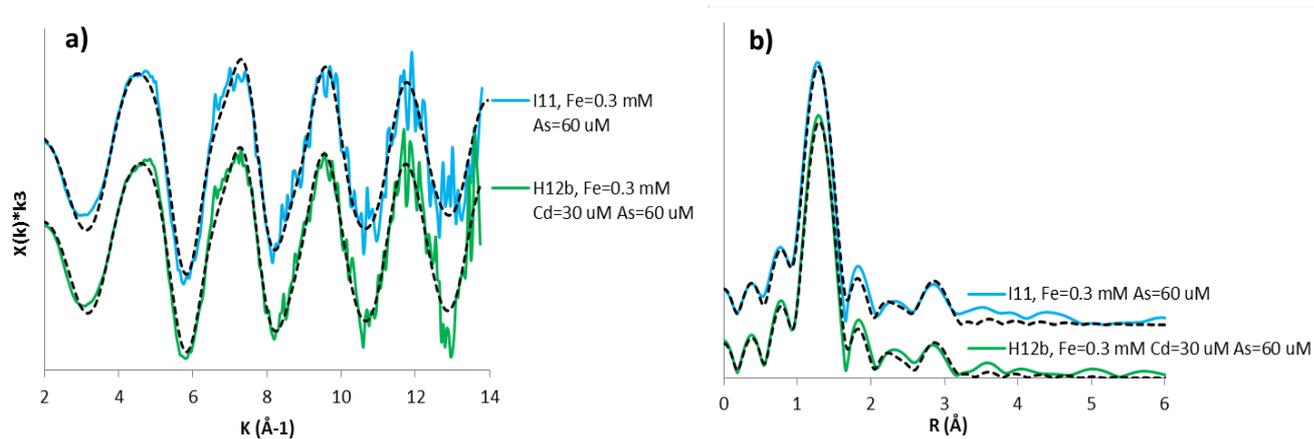
Fig S5. Results from EXAFS-measurements (solid lines) and models (dashed lines) at the As K edge. a) EXAFS spectra, b) Fourier transforms.
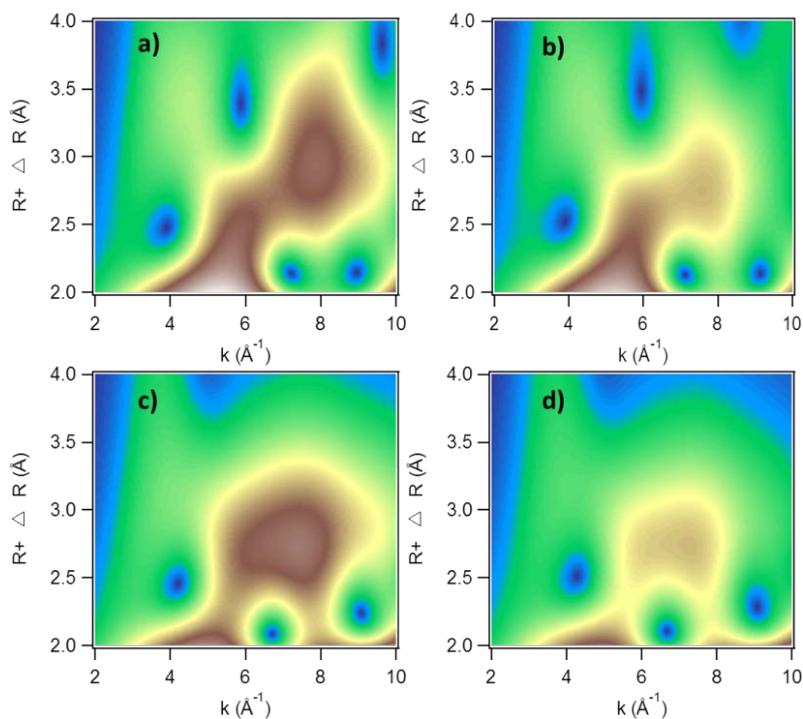
Fig S6. Wavelet transforms of EXAFS spectra and models for arsenic adsorbed to ferrihydrite. The *k*-range used was 3.6-12.5 Å^{-1} for all samples. a) Spectrum I11; 60 µmol L^{-1} As, 0.3 mmol L^{-1} Fe, b) Spectrum H12b; 60 µmol L^{-1} As, 0.3 mmol L^{-1}Fe, 30 µmol L^{-1} Cd, c) Model I11, d) Model H12b.